PAPER • OPEN ACCESS

Controlled inlet airflow in ventilated facades: a numerical analysis

View the article online for updates and enhancements.

Controlled inlet airflow in ventilated facades: a numerical analysis

M Pergolini[1,*], G Ulpiani[2], O Shehi[1], C Di Perna[2], F Stazi[1]

[1] Department of Materials, Environmental Sciences and Urban Planning (SIMAU), Polytechnic University of Marche, Ancona, Italy
[2] Department of Industrial Engineering and Mathematical Sciences (DIISM), Polytechnic University of Marche, Ancona, Italy
[*] m.pergolini@hotmail.it

Abstract. A research study was conducted to investigate the summer thermal performance of different ventilated façades, by means of experimentally validated numerical simulation. Three ventilated configurations were tested: L, with a lightweight external layer, IM and EM with a massive cladding respectively in the inner and outer side of the air cavity. TRNSYS was used to simulate the thermal behaviour of the façades. Five increasing air speeds were imposed at the inlet (from 0.2m/s to 2m/s). Air temperature and heat flux trends, at different wall positions, were surveyed. The experimentation was carried out on a lightweight and hyper-insulated mock-up in Central Italy. The airflow rate at the inlet was controlled by means of pulse width modulation (PWM) controlled axial fans installed on top of the air gaps. Temperature, air velocity, and thermal flux measurements were collected to validate the model. Simulation results were later post-processed by means of linear regression analysis. As expected, as the airflow speed increased, the air temperature within the cavity gradually and asymptotically decreased. With air speeds above 1.6 m/s, the cavity temperatures in the massive configurations EM and IM settled at around the same value. Further investigation regarded the comparison of the heat flux profiles. The EM prototype was found to outperform the others since it more effectively prevented the heat from entering the test room and allowed a significant heat share to be released, too.

1. Introduction

Ventilated skins are made of three functional layers (from the internal to the external side): insulation layer connected to the load-bearing structure; ventilation chamber connected to the outdoors by lower and upper openings; outer cladding supported by steel brackets.

Nowadays, such solutions are acknowledged to be effective cooling passive strategies, guaranteeing over 40% less incoming heat flux with respect to the unventilated configuration [1-3], improving the indoor microclimate and reducing the heating/cooling consumptions. This is especially true in presence of high solar radiation, as in Southern Europe [4].

The main climate-related parameters that influence the air gap behavior, and thus the energy performance of ventilated skins, are: geographical location [5], solar radiation [6] and wind speed [1]. The thermal behavior of ventilated solutions is also affected by components design features, such as height and width of the air gap [2], material of the external cladding [7], typology of joints (open [8] or closed [9]).

Integrated systems (ventilated facades mated with controlled airflow) have gained prominence in recent years. The ventilation source can be either outdoor air or indoor exhaust air. The first setup was analytically investigated by Astorqui et al. [10], who analyzed the potential of adding a second air chamber parallel to the existing one, fit with a device, at the top, to regulate the air flow. Other studies focused on the second setup: in [11], for instance, the authors proposed a mechanically ventilated facade equipped with an air-to-air heat exchanger between the outdoor air and the saturated exhaust air

extracted from within the building. A third solution is represented by hollow block ventilated walls, in which the cavity of the wall is the actual ventilation duct with controlled airflow [12].

In any case, experimental evidence substantiates how the air velocity in the cavity greatly influences the thermal performance [13]. Further investigation is required to fully unveil its role.

This research aims to bridge the gap by comparing the summertime behavior of three different types of ventilated facades under five controlled different airflow boundary conditions. A numerical model in TRNSYS is used for scenario analysis, once experimentally validated.

2. Numerical model

The modelling process of the case study comprised several steps. Three types of ventilated skins (Fig.1a) were applied to the west façade of an existing mock-up: the first configuration (L) represented a lightweight solution and featured negligible mass. It was conceived with an aerated gap enclosed by a white plastered OSB panel. It served as reference case for comparisons. The second configuration (IM) exhibited a massive layer adjacent to the insulation material. The external gap was enclosed by a plastered OSB panel. In the third configuration (EM), the mass was external, finished with external white plaster. The geometrical features of the test room were defined in a 3D model, using SketchUp software (Fig.1b). The 1x 2.30 m^2 façades enclosed a single thermal zone with no glazed surfaces and rectangular in plan (net floor area of 12 m^2). CLT panels were used for the load-bearing structure, covered by a wooden pitched roof.
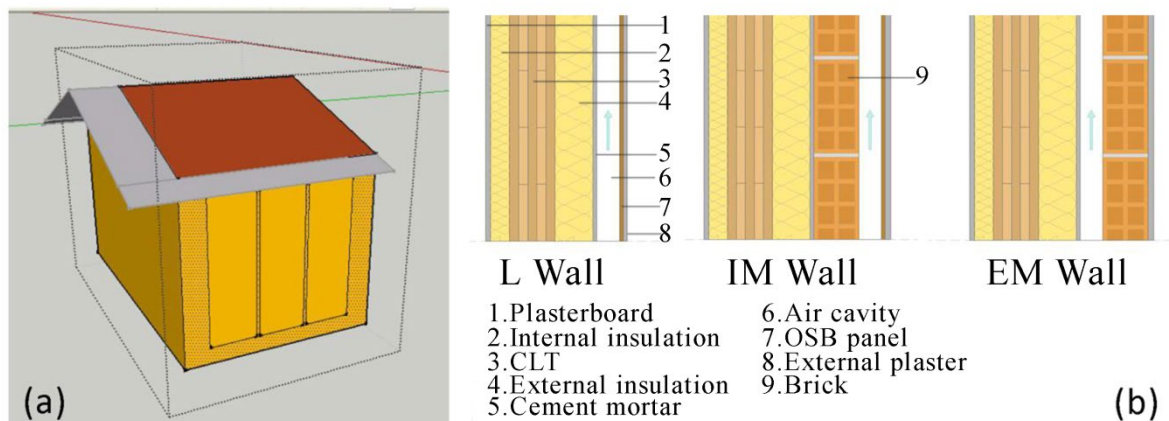

Figure 1. (a) Test room model in SketchUp and (b) layers succession of the three prototypes.

The hourly weather file was generated by Meteonorm for the municipality of Agugliano (43°32'23.1''N, 13°22'14.7''E; 137 m a.s.l.), featuring Cfa climate according to Koppen and Geiger [14]. The 3D-model and weather file were then imported in TRNSYS-17. The effect of the air cavity was attained by coupling the thermal response of building component Type 56 (by specifying real walls composition and room thermal parameters) and the ventilated air cavity façade Type 1230. Type 1230 models an external massive wall with a ventilated air gap behind it. It is based on the heat transfer principles and algorithms for solar energy storage developed by Duffie et al. [15]. The back side of the air gap is a small resistive layer, whose temperature and thermal resistance are coupled with Type 56 wall for modeling the interior wall heat transfer. Figure 2 shows how the boundaries of Type 56 and Type 1230 overlap, by matching the outermost wall layer (typically insulation) with the inner side of the cavity. Type 1230 accepts the backside temperature of this layer from Type 56 and returns the temperature on the interior surface of the air gap, while Type 56 accepts this boundary temperature from Type 1230 and returns the surface temperature of its exterior wall. The model is derived from energy balances on the massive wall, the air stream, the exterior surface, and the interior surfaces.
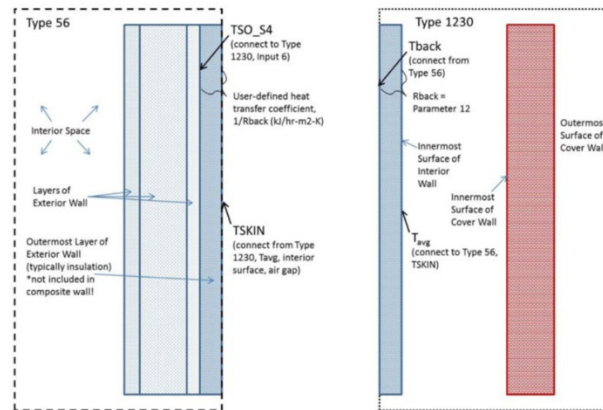
Figure 2. Modeling boundaries of Type 1230 [16].

Five increasing levels of inlet airflow rates were assumed, as reported in Table 1, starting from a minimum value of 0.2 m/s, representative of natural ventilation and assuming four increasing steps of 0.5 m/s. The external convective heat transfer coefficient was 64 kJ/(hm^{2}K), typical of ventilated surfaces [16].

Table 1. Airflow input.

Inlet airflow speed (m/s)	0.2	0.5	1	1.5	2
Inlet airflow rate (kg/h)	42.34	105.84	211.68	317.52	423.36

3. Model validation

The three ventilated prototypes were realized on the west-oriented façade of the mock-up.

The inlet air speed at the openings was regulated by means of a set of pulse-width modulation (PWM) controlled DC fans. 13 fans were installed on top of each air duct and connected in series to the power supply. High-speed fans were selected, with nominal dimensions of 60 x 60 x 25 mm^3 and maximum airflow rate of 67 m^3/h (Figure 3a).
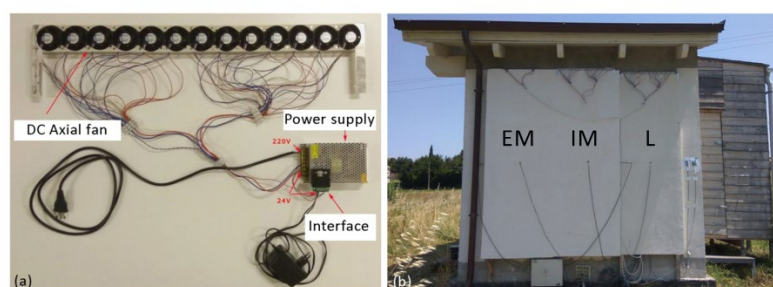

Figure 3. (a) DC fans with PWM control set-up and (b) corresponding prototypes.

The power input was regulated by a controller that translated the analogue voltage input to an equivalent PWM signal. The whole system was supervised through a customized LabVIEW Virtual Instrument. Figure 3b shows the ventilated prototypes and the control apparatus.

The monitoring campaign lasted a month (May). The external boundary conditions (wind speed and direction, outdoor temperature and relative humidity) were monitored by a weather station close to the mock-up, whereas the surface temperatures on the external wall and on the inner side of the air gap were detected at 115 cm height. Data were recorded at 1-minute intervals.

Experimental data were analysed in order to validate the model. As shown in Figure 4, the ratio between the experimental and the simulated values of the surface temperature in the inner sides of the ventilated facades fell within the limits of acceptable uncertainty. However, it should be clarified that the configurations L and IM are the ones in which the simulated values diverge more from the experimental ones. This is attributable to the fact that the TYPE 1230 assumes a massive layer (such as clay, bricks or wood) as external cladding. Therefore, the error range for an external lightweight massive cladding is higher.
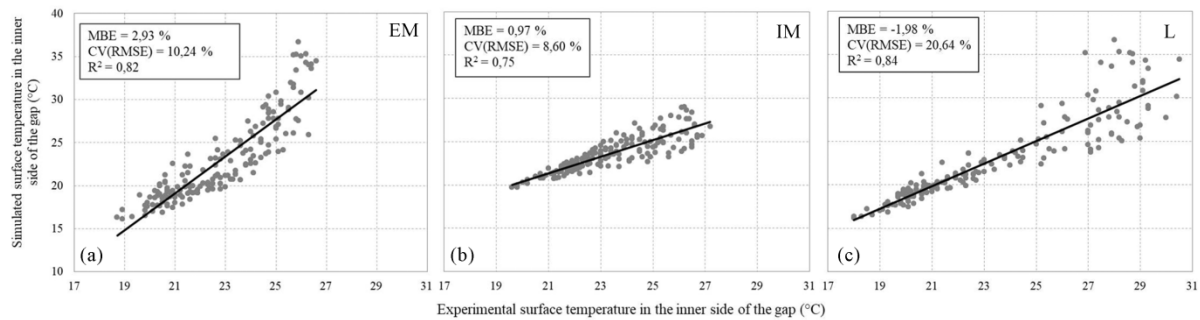

Figure 4. Results validation for (a) EM, (b) IM, and (c) L walls.

4. Numerical results

Figure 5 presents the surface temperature trends on the inner side of the ventilated gaps (at 115 m height) for all the ventilated skins. The values refer to a single summer day, considering the minimum (0.2 m/s) and maximum (2 m/s) air speed at the inlet.

The lightweight configuration L was affected by the ventilation increase only during the central day hours, with a temperature reduction of around 3°C over peak hours. The IM surface temperature dropped by 1.5°C, during the day and night, whereas EM's exhibited a different thermal profile: in the morning, the heated outer mass warmed up the innermost side of the gap, while after 15:00, it stayed much cooler due to the combined effect of the higher airflow and cooling of the outmost surface. This was especially noticeable for increasing air speed levels.

A linear regression analysis was conducted on the TRNSYS simulations outputs to gain better knowledge of the relation between the surface temperatures on the inner side of the gaps and the airstream speed (Figure 6). As expected, the air temperature within the cavity gradually and asymptotically decreased as the airflow speed was incremented. Above a threshold value of 1.6 m/s, the temperature of the massive solutions, EM and IM, equalized. Conversely, for lower airstream speeds, typical of residential and commercial buildings, the position of the thermal mass caused significant temperature variations, thus influencing the incoming heat flux. Therefore, the heat fluxes of the three walls, both on their inner side of the cavity and in the internal side of the wall were analyzed.
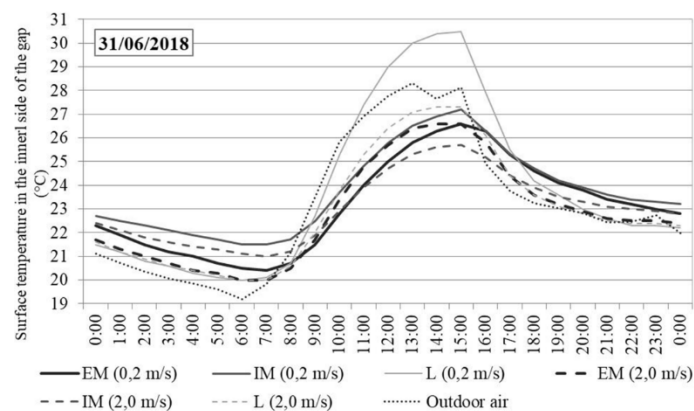

Figure 5. Internal surface temperatures of the three configurations plotted for a single summer day, considering two air speeds

$$y = 0.5909x^4 - 3.0099x^3 + 5.5451x^2 - 4.5916x + 23.374$$
$$y = 0.4511x^4 - 2.311x^3 + 4.2637x^2 - 3.5221x + 22.864$$
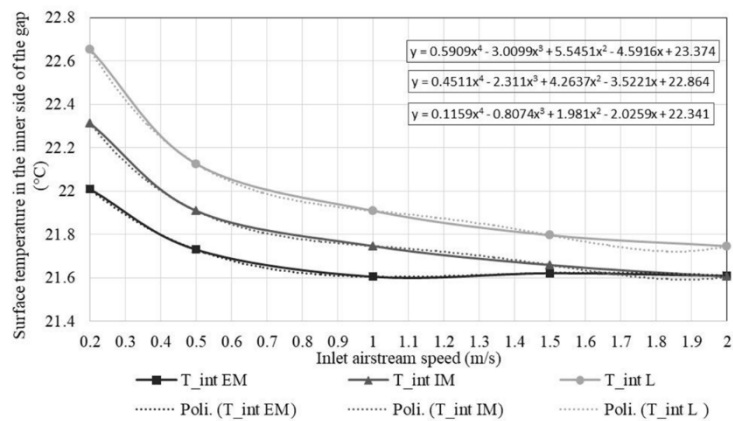$$y = 0.1159x^4 - 0.8074x^3 + 1.981x^2 - 2.0259x + 22.341$$

Figure 6. Linear regression of the inner surface temperature of the gap for different air speeds.

Figure 7 shows the daily average fluxes, considering two airflow rates, and assuming, with positive sign, the fluxes with incoming direction towards the mock-up. For EM wall, the air speed had scarce influence on the fluxes while, for the other two, the heat fluxes declined by raising the air velocity.

The relation between the heat fluxes on the internal side of the walls and the five levels of inlet airflows is reported in figure 8. The variation, for massive solutions, was around 1 W/m² before taking an asymptotical shape, thus demonstrating a reduced influence of the air speed level. The inner mass (IM) emphasized the heat transfer toward the indoors. Conversely, the outer mass acted as a thermal buffer between the outdoors and the gap, thus minimizing the incoming heat fluxes.

Overall, the EM configuration was found to be the best solution in reducing the ingoing and outgoing heat transfer, regardless of the airflow rate.
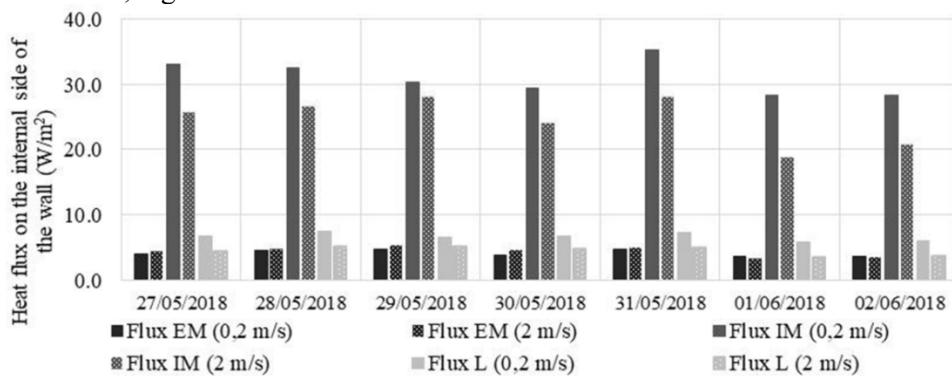

Figure 7. Daily average fluxes for maximum and minimum airflow rate.

$$y = 0.3187x^4 - 1.728x^3 + 3.4773x^2 - 3.2523x - 2.3018$$
$$y = 0.1593x^4 - 0.813x^3 + 1.5027x^2 - 1.2372x - 2.3603$$
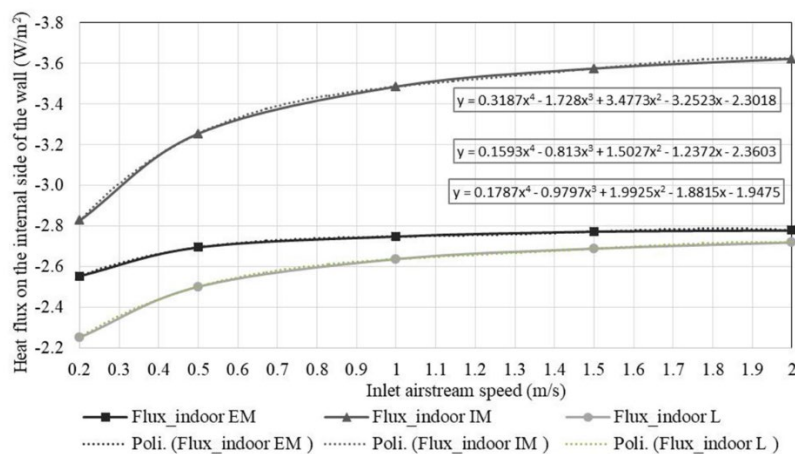$$y = 0.1787x^4 - 0.9797x^3 + 1.9925x^2 - 1.8815x - 1.9475$$

Figure 8. Linear regression of the indoor heat fluxes for different air speeds.

5. Conclusion

The thermal performance of three types of ventilated skins was numerically evaluated in summertime. The simulation model was created by using the energy software tool TRNSYS-17. Airflow parameters of the ventilated air cavity were simulated by imposing five increasing air speeds at the inlet. The model represented a test room located in Central Italy, equipped with the prototypes of the three ventilated skins and monitored in May. The airstream rates at the inlet were managed by means of PWM controlled axial fans placed on top of the air cavities. The model was calibrated referring to the meteorological variables (wind speed and direction and solar radiation) of the selected location. The numerical outcomes demonstrated that the EM solution, characterized by a massive layer on the outer cladding, represented the best practice in Mediterranean climates, by successfully limiting the incoming and outgoing heat fluxes through the envelope.

References

[1]   A. Gagliano, F. Nocera, and S. Aneli, "Thermodynamic analysis of ventilated facades under different wind conditions in summer period," *Energy Build.*, vol. 122, pp. 131–139, 2016.

[2]   C. Marinosci, P. A. Strachan, G. Semprini, and G. L. Morini, "Empirical validation and modelling of a naturally ventilated rainscreen fac building," *Energy Build.*, vol. 43, pp. 853–863, 2011.

[3]   F. Leccese and U. Pisa, "Cooling of buildings : energy efficiency improvement through ventilated structures," *WIT Transactions on Ecology and the Environment*, no. 62, pp.199-210, 2003.

[4]   C. Aparicio-Fernández, J. Vivancos, and P. Ferrer-Gisbert, "Energy performance of a ventilated façade by simulation with experimental validation," *Appl. Therm. Eng.*, vol. 66, no. 1–2, pp. 563–570, 2014.

[5]   M. R. D. A. Santiago and F. L. Peci, "Sensitivity study of an opaque ventilated façade in the winter season in different climate zones in Spain," *Renew. Energy*, vol. 75, pp. 524–533, 2015.

[6]   I. Guillén, V. Gómez-lozano, J. María, and P. A. López-jiménez, "Thermal behavior analysis of different multilayer fac Numerical model versus experimental prototype," *Energy Build.*, vol. 79, pp. 184–190, 2014.

[7]   F. Stazi, F. Tomassoni, A. Vegliò and C. Di Perna, "Experimental evaluation of ventilated walls with an external clay cladding", *Renew. Energy*, vol. 36, pp. 3373–3385, 2011.

[8]   C. Sanjuan and M. J. Sua, "Experimental assessment of the performance of open joint ventilated facades with buoyancy-driven airflow," *Sol. Energy*, vol. 91, pp. 131–144, 2013.

[9]   E. Giancola, M. J. Su, E. Blanco, and M. R. Heras, "Experimental evaluation of the airflow behaviour in horizontal and vertical Open Joint Ventilated Facades using Stereo-PIV," *Renew. Energy*, vol. 109, pp. 613–623, 2017.

[10]   J. Santa, C. Astorqui, and C. Porras-amores, "Ventilated Facade with double chamber and flow control device," *Energy Build.*, vol. 149, pp. 471–482, 2017.

[11]   C. Cianfrini, M. Corcione, E. Habib, and A. Quintino, "Energy performance of a lightweight opaque ventilated facade integrated with the HVAC system using saturated exhaust indoor air," *Energy Build.*, vol. 50, pp. 26–34, 2012.

[12]   J. Yu, J. Yang, and C. Xiong, "Study of dynamic thermal performance of hollow block ventilated wall," *Renew. Energy*, vol. 84, pp. 145–151, 2015.

[13]   J. Yu, H. Ye, X. Xu, J. Huang, Y. Liu, and J. Wang, "Experimental study on the thermal performance of a hollow block ventilation wall," *Renew. Energy*, vol. 122, pp. 619–631, 2018.

[14]   A. S. Nouri, J. P. Costa, M. Santamouris, and A. Matzarakis, "Approaches to outdoor thermal comfort thresholds through public space design: A review," *Atmosphere (Basel).*, vol. 9, no. 3, 2018.

[15]   J. A. Duffie and W. A. Beckman, "*Solar Enginering of Thermal Processes Solar Engineering",* Fourth Edition.

[16]   Tess Component Libraries 17, "Ventilated cavity façade"Tess Libraries," pp. 1–79.